HHS Public Access

Author manuscript

Environ Microbiol. Author manuscript; available in PMC 2015 June 15.

Published in final edited form as:

Environ Microbiol. 2013 August ; 15(8): 2238–2253. doi:10.1111/1462-2920.12095.

A spider web strategy of type IV pili-mediated migration to build a fibre-like Psl polysaccharide matrix in *Pseudomonas aeruginosa* biofilms

Shiwei Wang[1], **Matthew R. Parsek**[3], **Daniel J. Wozniak**[2,**], and **Luyan Z. Ma**[1,*]

[1]State Key Laboratory of Microbial Resources, Institute of Microbiology, Chinese Academy of Sciences, Beijing 100101, China.

[2]Department of Microbial Infection and Immunity, Department of Microbiology, Center for Microbial Interface Biology, The Ohio State University, Columbus, OH 43210, USA.

[3]Department of Microbiology, University of Washington, Seattle, WA, USA.

Summary

Bacterial motilities participate in biofilm development. However, it is unknown how/if bacterial motility affects formation of the biofilm matrix. Psl polysaccharide is a key biofilm matrix

*correspondence. luyanma27@im.ac.cn; Tel. (+86) 10 62562753; Fax (+86) 10 62562753. **daniel.wozniak@osumc.edu; Tel. (+1) 614 247 7629; Fax (+1) 614 292 9616.

Supporting information

Additional Supporting Information may be found in the online version of this article at the publisher's web-site:

Fig. S1. The fibre-like Psl strands connecting multiple-cell aggregates/microcolonies at biofilm initiation. Shown are bio-films of PAO1 and WFPA801 after 22 h of growth under flow condition and stained with HHA-FITC (green, Psl matrix) and FM4-64 (red, bacteria membrane stain). Black arrows indicate the Psl fibres present in the area with a few bacteria. Scale bar, 5 μm.

Fig. S2. The formation of the Psl-fibre matrix is not required for the production of Pel and alginate. Shown are biofilms of MJK8 (A), MJK8/D*pel* (B), MJK8/D*psl* (C), PAO1 (D), WFPA1 (E) and WFPA802 (F) after 22 h of growth under flow condition and stained with HHA-FITC (green, Psl matrix) and FM4-64 (red, bacteria membrane stain). The lower right image in each biofilm panel is the merge of corresponding red and green images. Grey images are DIC image of biofilms. Bar, 2 μm for MJK8 and MJK8/Δ*pel*, 10 μm for MJK8/Δ*psl*, 2 μm for WFPA1 and 5 μm for PAO1.

Fig. S3. The radial pattern Psl-fibre matrix was located at the stalk area of MSBS. Shown was a selected optical CLSM section of a Δ*fliC* biofilm. The blue line on the rectangle image shows the section located at the stalk of MSBS, which is depicted in the large square. Arrows indicate the MSBS (square) and the locationofthe radial Psl-fibre matrix within the MSBS (rectangle image). Red: Psl matrix; Green: Bacteria.

Fig. S4. The Psl matrix in the pellicles of PAO1, Δ*pilA*, and Δ*fliM*Δ*pilA* strains. Shown are selected CLSM images located in the middle of pellicles. The pellicles were stained by FITC-HHA for Psl matrix (green) after 44 h of growth under a static growth condition. Grey image was the corresponding DIC image of biofilm. Scale bar, 5 μm.

Fig. S5. Comparison of Psl released into PBS buffer and Jensen's media from mid-log phase bacteria of T4P mutants and *relA spoT* deletion mutant during 4 h of incubation at RT. Released Psl and bacterial surface-bound Psl were detected by immunoblotting with anti-Psl serum.

Fig. S6. Concentrated Psl polysaccharide (green) and eDNA (red) were presented in the centre of a radial pattern Psl fibre matrix. Shown are selected CLSM images located in the middle of pellicles. The pellicle of Δ*fliC* strain was stained by FITC-HHA for Psl matrix (green) and PI for eDNA/dead cells after 44 h of growth under a static growth condition. Grey image was the corresponding DIC image of biofilm. Arrows indicate the colocalized Psl and eDNA in the centre of the radial pattern Psl fibre matrix. Scale bar, 5 μm.

Fig. S7. The twitching zone of PAO1 and *pilA* mutant on the Jensen's media and PBS agar plate. The hole in the middle is the inoculation hole. The red colour is the result of tetrazolium red stain. The diameter of twitching zone was measured by addition of distance a and b as depicted in the middle image. Scale bar, 7 mm. * indicates statistically significant difference between measurements ($P < 0.007$, *t*-test). TZ, Twitching Zone.

Video S1. How the radial pattern Psl-fibre matrix maintain the biofilm structure of a Δ*fliC* strain. Shown was a serial optical CLSM section of a Δ*fliC* biofilm from substratum to the top of biofilm. Red: Psl matrix; green: bacteria in the biofilm.

component of *Pseudomonas aeruginosa*. Here we report that type IV pili (T4P)-mediated bacterial migration leads to the formation of a fibre-like Psl matrix. Deletion of T4P in wild type and flagella-deficient strains results in loss of the Psl-fibres and reduction of biofilm biomass in flow cell biofilms as well as pellicles at air-liquid interface. Bacteria lacking T4P-driven twitching motility including those that still express surface T4P are unable to form the Psl-fibres. Formation of a Psl-fibre matrix is critical for efficient biofilm formation, yet does not require flagella and polysaccharide Pel or alginate. The Psl-fibres are likely formed by Psl released from bacteria during T4P-mediated migration, a strategy similar to spider web formation. Starvation can couple Psl release and T4P-driven twitching motility. Furthermore, a radial-pattern Psl-fibre matrix is present in the middle of biofilms, a nutrient-deprived region. These imply a plausible model for how bacteria respond to nutrient-limited local environment to build a polysaccharide-fibre matrix by T4P-dependent, bacterial migration strategy. This strategy may have general significance for bacterial survival in natural and clinical settings.

Introduction

Biofilms (surface-associated bacterial communities) are found in virtually every habitat. In natural and clinical settings, biofilms enhance survival, enabling organisms to adapt to changing conditions collectively instead of as single cells (Costerton *et al.*, 1995). Biofilm growth is also correlated with starvation-induced tolerance to antibiotics *in vivo* (Costerton *et al.*, 1999; Lewis, 2007; Nguyen *et al.*, 2011). Bacterial communities mainly rely on extracellular matrix to enmesh bacteria and maintain biofilm structure and integrity (Sutherland, 2001; Whitchurch *et al.*, 2002a; Matsukawa and Greenberg, 2004; Friedman and Kolter, 2004a; Ma *et al.*, 2006; 2009; Kolodkin-Gal *et al.*, 2012). Bacterial motility was reported to contribute to biofilm architecture and development (O'Toole and Kolter, 1998; Klausen *et al.*, 2003a; Shrout *et al.*, 2006; 2011; Conrad *et al.*, 2011). However, it is not clear whether bacterial motility is involved in formation of the biofilm matrix and if there is any link between bacterial migration and biofilm matrix formation.

Exopolysaccharides are a key biofilm matrix component of many Gram-positive and -negative bacteria, as they contribute to the overall biofilm architecture and resistance (Mah *et al.*, 2003; Matsukawa and Greenberg, 2004; Friedman and Kolter, 2004a; Ma *et al.*, 2006; 2009; Flemming and Wingender, 2010; Colvin *et al.*, 2011; Yang *et al.*, 2011; Kolodkin-Gal *et al.*, 2012). *Pseudomonas aeruginosa*, a Gram-negative environmental bacterium, is a model organism for studying biofilms. It is also an important opportunistic pathogen that can cause lethal acute and chronic persistent infections in cystic fibrosis (CF) patients and individuals with a compromised immune system. *P. aeruginosa* can form biofilms on a variety of abiotic and biotic surfaces such as the mucus plugs of the CF lung, contaminated catheters and contact lenses (Davies *et al.*, 1998; Singh *et al.*, 2000; Willcox, 2007). It can also form pellicles at the air-liquid interface of standing cultures as does the Gram-positive bacterium *Bacillus subtilis* (Friedman and Kolter, 2004b; Kolodkin-Gal *et al.*, 2010). Three exopolysaccharides, alginate, Psl and Pel, are involved in *P. aeruginosa* biofilm formation (Hentzer *et al.*, 2001; Friedman and Kolter, 2004b). *P. aeruginosa* cells often become mucoid upon prolonged colonization of the CF lung. The mucoid phenotype is due to the overproduction of alginate that provides an advantage for *P. aeruginosa* in the airway of CF

patients (Govan and Deretic, 1996). Pel is a glucose-rich exopolysaccharide, which is required to form air-liquid interface biofilms (pellicles) (Friedman and Kolter, 2004b). Psl is a repeating pentasaccharide containing D-mannose, D-glucose and L-rhamnose (Byrd *et al.*, 2009). This exopolysaccharide is an essential matrix component for non-mucoid and mucoid *P. aeruginosa* to initiate and maintain biofilms (Matsukawa and Greenberg, 2004; Ma *et al.*, 2006; 2009; 2012; Yang *et al.*, 2012). Data from Yang and colleagues suggest that Psl is more important than Pel in *P. aeruginosa* PAO1 biofilm microcolony formation and antibiotic resistance (Yang *et al.*, 2011). Our previous studies showed that Psl is arranged in a helical pattern on the bacterial surface and forms fibre-like strands that connect each other to enmesh bacteria in a biofilm (Ma *et al.*, 2009). Overproduction of Psl enhances bacteria-bacteria interaction and results in more mushroom-shaped biofilm structure (MSBS) in a flow cell chamber (Ma *et al.*, 2006). However, it is not clear how the fibre-like Psl strands form, and whether the Psl-fibre strands are important to build the matrix and biofilm structure. It is also unknown whether the formation of the Psl-fibre matrix depends on other exopolysaccharides of *P. aeruginosa*.

It is reported that bacterial motility affects biofilm formation and architecture (O'Toole and Kolter, 1998; Chiang and Burrows, 2003; Klausen *et al.*, 2003a; Shrout *et al.*, 2006; 2011). Bacteria can move on surfaces via distinct appendage-specific motility modes. Flagella mediate bacterial swimming and surface-bound spinning (Conrad *et al.*, 2011). Flagella and type IV pili (T4P) mediate swarming, a motility mode used for colony expansion along a semisolid surface (Kohler *et al.*, 2000). T4P also mediate twitching that is commonly observed in dense aggregates with cell-to-cell contact (Whitchurch, 2006). The T4P on the bacterial cell works by extension and retraction of the pili to pull the cell forward (Skerker and Berg, 2001; Bertrand *et al.*, 2010). In *P. aeruginosa*, the polar flagella and T4P are both located at the same cell pole, but drive bacteria in opposite directions (Conrad *et al.*, 2011). Flagella and T4P-mediated motility are both important to build a biofilm structure *in vitro* (Klausen *et al.*, 2003a,b). T4P are important for the formation of the MSBS cap (Barken *et al.*, 2008). Barken and colleagues suggested that T4P might function as niche-specific adhesins/matrix components in *P. aeruginosa* biofilms (Barken *et al.*, 2008). O'Toole and colleagues have also reported that T4P play an important role in microcolony formation while flagella have a role in the initial cell-to-surface interaction (O'Toole and Kolter, 1998). In *Myxobacteria*, extracellular polysaccharides are an anchor for T4P, triggering pili retraction and enabling social motility (Mauriello *et al.*, 2010). In *P. aeruginosa*, it is unclear whether there is a link between bacteria motility and exopolysaccharide.

In this study, we use non-destructive *in situ* detection technique to investigate whether T4P/flagella and their directed motility affect the exopolysaccharide matrix in *P. aeruginosa* biofilms, how a fibre-like Psl matrix is formed, and the contribution of the Psl-fibres to biofilm formation. Our data show that T4P-mediated bacterial migration is critical for the formation of a Psl-fibre matrix in biofilms and reveal that the Psl-fibre matrix is formed through a strategy similar to the spider web formation. We also provide a fundamental and significant understanding about how bacteria respond to nutrient-poor environments to maintain its community structure.

Results

The fibre-like Psl polysaccharide strands in the biofilms of *P. aeruginosa* PAO1-derived strains

Our previous study showed that *P. aeruginosa* can form fibre-like Psl strands enmeshing bacteria within a biofilm (Ma *et al.*, 2009). The Psl-fibre strands were present in the biofilm of both *P. aeruginosa* wild type strain PAO1 and Psl-inducible strain WFPA801 and most clearly visualized at the early stages of biofilm development (Figs 1A and S1). The Psl-fibres with a strong fluorescent signal were observed in the biofilm of WFPA801, surrounding the multiple-cell aggregates, connecting microcolonies, and forming a spider web-like matrix (Fig. S1). Strikingly, many Psl-fibres were present at areas where there were few bacteria (indicated by arrows in Fig. 1A and Fig. S1). Thus, these Psl-fibre strands did not appear to be formed by bacterial cell–cell interaction as we assumed previously (Ma *et al.*, 2009). To investigate whether the similar phenomenon is present in other PAO1-derived strains, and whether the other polysaccharides produced by *P. aeruginosa* affect the formation of the Psl-fibre matrix, we examined a rugose small-colony variant (RSCV) derived from a laboratory-grown biofilm of PAO1, MJK8 and its isogenic *pel* and *psl* mutants (Table 1) (Kirisits *et al.*, 2005). Growth of *P. aeruginosa* in biofilms and chronic CF airway infections produces RSCVs (Starkey *et al.*, 2009). Both clinical and *in vitro* derived biofilm RSCVs display increased production of the Pel and Psl polysaccharides and an elevated capacity to form biofilms (Starkey *et al.*, 2009). Psl staining showed that the fibrelike Psl was also found in the biofilm of MJK8 and was clearly visualized at the area with few bacterial cells (Fig. 1B, white arrow). No staining was present in the MJK8 *psl* mutant (Fig. S2). The Psl matrix in the biofilms of MJK8 and MJK8Δ*pel* was indistinguishable (Fig. S2), indicating that formation of the Psl-fibre matrix is independent of Pel.

To determine whether the formation of Psl-fibres required alginate, we constructed WFPA802, a Psl-inducible strain in an alginate synthesis deficient background (Table 1). The Psl-fibres were observed in the biofilm of WFPA802 (Fig. 1B) and the Psl matrix of WFPA802 (Fig. S2F) was similar to WFPA801 (Ma *et al.*, 2009). In addition, the Psl matrix of an alginate-synthesis-deficient strain, WFPA1 (Fig. S2E) was also similar to that of the wild type strain PAO1 (Fig. S2D). Taken together, these data showed that RSCV MJK8, Pel-deficient RSCV, and alginate-deficient strains can form the Psl-fibres, indicating the formation of the Psl-fibre matrix does not require Pel polysaccharide or alginate.

The formation of Psl-fibre matrix depends on T4P, but not flagella

Previous reports showed both flagella and T4P were important for biofilm development (Klausen *et al.*, 2003a). Recently, we found that non-motile mucoid strain FRD1 did not form the fibre-like Psl strands (Ma *et al.*, 2012), tempting us to hypothesize that motility may be involved in the formation of the Psl-fibre. To test this, we first examined the Psl-fibre matrix formation of a PAO1-derived *fliC* (encodes flagellin, the main subunit of flagellum) deletion mutant, which lacks bacterial surface flagella and flagella-mediated motility (Klausen *et al.*, 2003b). After 4-day growth in a flow chamber, the *fliC* mutant formed a similar flat biofilm (25 ± 5 μm thickness) as compared with that of wild type

PAO1, which covered the entire chamber surface (Fig. 2A). However, biofilms formed by the *fliC* mutant had few MSBS but some irregular-shaped large macrocolonies were visible as white spots in the flow chamber (Fig. 2A, C and E). Strikingly, the *fliC* mutant showed extensive fibre-like Psl strands (Fig. 2C, red panel) forming a radial-pattern matrix with Psl-fibres coming out from a centre where there was concentrated Psl material. This radial Psl-fibre matrix was clearly observed in the middle of biofilm, connecting microcolonies, and continued for a few micrometers within a biofilm (Fig. 2E and Video S1). The similar radial matrix pattern could be observed in the biofilms of the wild type (Fig. 2B), but was more pronounced in the *fliC* mutant. This revealed that the generation of Psl-fibre matrix did not require flagella.

To investigate whether T4P or T4P-mediated bacterial migration is involved in the formation of the radial Psl-fibre matrix within the biofilms, we utilized a *fliM* and *pilA* double deletion mutant, which lacked T4P-mediated motility and flagella-mediated motility (Klausen *et al.*, 2003b). After 4-day growth in a flow chamber, the biofilm of the Δ*fliM*Δ*pilA* strain was mainly composed of thin multicellular aggregates (thickness approximately 10 μm) that were not readily observed in the flow chamber (Fig. 2A). Furthermore, no clear fibre-like Psl structures or typical biofilm matrix patterns were observed in the biofilm of the Δ*fliM*Δ*pilA* strain (Fig. 2D). Loss of Psl fibres was not due to the reduction of Psl in the biofilm because there was more Psl in the biofilm of Δ*fliM*Δ*pilA* than that of PAO1 and *fliC* mutant according to *COMSTAT* analysis (indicated by the number above each panel in Fig. 2B–D). To determine if mutation of T4P are sufficient to account for the loss of the fibre-like Psl structure, we examined the biofilm of Δ*pilA* strain since PilA is the major structural subunit of T4P and is essential for T4P-mediated twitching motility (Table 1) (Whitchurch, 2006). Compared with the biofilm of wild type PAO1 strain, Δ*pilA* bacteria formed a few microcolonies with concentrated Psl, which appeared fibre-less especially at the middle to the top of the microcolonies (Fig. 3). As *pilA* mutants cannot generate a Psl-fibre matrix, indicating the formation of a Psl-fibre matrix required T4P.

In MSBS, the radial Psl-fibre matrix was located at the stalk area above the substratum (Fig. S3). This suggested that formation of the radial Psl-fibre matrix did not rely on the adherence on a solid surface. Consistent with this, we observed a similar radial pattern Psl-fibre matrix in an air-liquid interface biofilm (pellicle) of the *fliC* mutant grown under static conditions (Fig. 4). This indicated that the radial-pattern Psl-fibre matrix can be formed in the biofilm grown under either flow or static conditions.

Type IV pili-mediated bacterial migration builds a Psl-fibre matrix

To determine whether formation of the Psl fibre matrix required the presence of T4P structure or T4P-mediated motility, we utilized three pilus-retraction-deficient strains, Δ*pilT*, Δ*fliC*Δ*pilT* and Δ*pilH* (Table 1) (Bertrand *et al.*, 2010). As controls, we also examined Δ*fliC*, Δ*pilA* and Δ*fliM*Δ*pilA* strains. Since Psl-fibre matrix can form in pellicles, we grew pellicles to examine the Psl matrix of above mutant strains. All these strains were able to form pellicles at air-media interface with various biofilm bio-masses after 2-day growth (Fig. 4). The Psl staining results did show a correlation between T4P-mediated motility and the Psl-fibre formation in pellicles. The Δ*fliC* strain retained T4P-mediated twitching motility at a

level similar to wild type strain (Table 1) and this strain can form a typical radial Psl-fibre matrix in pellicles and flow-cell biofilms (Figs 4, 2C, and 2E). The *pilT* and *pilH* genes are both involved in pilus retraction in *P. aeruginosa*. PilH is a CheY-like response regulator, which interacts with ATPase PilT to mediate pilus retraction (Bertrand *et al.*, 2010). Deletion of either *pilT* or *pilH* results in increased levels of surface T4P relative to wild type, yet Δ*pilT* strains were completely defective for twitching motility and Δ*pilH* bacteria retained some twitching motility (Table 1) (Bertrand *et al.*, 2010). Consistent with the phenotype of twitching motility, Psl staining results showed that the D*pilH* strain can form Psl-fibre structure in pellicle (Fig. 4). However, no typical Psl-fibres were found in the pellicle of Δ*pilT* and Δ*fliC*Δ*pilT* strains, which had totally loss of twitching motility (Fig. 4). Similar fibreless Psl matrixes were found in the pellicles of Δ*pilA* and Δ*fliM*Δ*pilA* strains that lacked T4P and T4P-mediated twitching motility (Fig. S4). Since the Δ*pilT* and Δ*fliC*Δ*pilT* strains retain surface expression of T4P yet lack twitching motility and biogenesis of the Psl-fibres, this result indicates that T4P-mediated motility, but not T4P structure, plays a key role for the formation of a Psl fibre matrix.

The contributions of Psl-fibres in *P. aeruginosa* biofilm formation

Neither the *pilA* mutant nor the *fliMpilA* double mutant can form the Psl-fibres (Fig. S4). The flow cell biofilms derived from these strains also had much less biomass compared with Psl-fibre-proficient strains PAO1 and Δ*fliC* (Figs 2 and S4). The hyperpiliated strains Δ*pilT* and Δ*fliC*Δ*pilT* also cannot form the Psl-fibres, and their biofilm had little biofilm biomass in a flow cell chamber as that of the *pilA* mutants (Figs 5A and 2A). These suggested that the Psl-fibres had contributions on the maintaining of biofilm biomass. Furthermore, there are more Psl presented in the microcolonies of Δ*pilA* strain than PAO1 microcolonies according to the fluorescent intensity of Psl (Fig. 3). Psl signal per μm^3 biofilm biomass of Δ*pilA* microcolonies was sixfold higher than PAO1 (the right panels of Fig. 3 and compare the number on the upper right corner in each image). Independently, Yang and colleagues also detected a large amount of matrix material in the flow cell biofilm of *pilA* mutant (Yang *et al.*, 2011). In addition, the *fliMpilA* mutant also had more Psl relative to its biofilm biomass, compared with that of PAO1 and *fliC* mutant (Fig. 2B – D). This suggested that the Psl-fibre-deficient strains, such as *pilA* mutants, required more Psl to keep biomass in a microcolony than the Psl-fibre-proficient strains (Fig. 3). This also implied that forming Psl fibres may be an efficient way for bacteria to occupy a surface and build the biofilm biomass, which allows bacteria to use less Psl to gain more biomass. These data suggested that the formation of Psl-fibres was important for efficient biofilm formation.

The Psl-fibre matrixes were also located at the stalk area of MSBS (Fig. S3), suggesting their potential contributions to the formation of MSBS, perhaps serving as a focal point for T4P-mediated motility to form a MSBS cap. Consistently, Δ*pilA* and Δ*fliM*Δ*pilA* were unable to form typical MSBS with mushroom-shaped caps (Barken *et al.*, 2008; Yang *et al.*, 2011). In contrast, Δ*pilH* bacteria retained the ability to form Psl-fibres in a pellicle biofilm (Table 1 and Fig. 4), which can also form mushroom-shape caps with minor defects in a flow-cell biofilm as reported previously (Barken *et al.*, 2008). Taken together, these data suggested the formation of Psl-fibres were critical for maintaining the biomass and three-dimensional structure of biofilm.

The Psl-fibre matrixes were also observed in the middle of pellicles formed at the air-media interface during static growth, leading us to investigate the contribution of Psl-fibre in the pellicle formation. We grew pellicles at air-media interface for 20 h, and then compared the pellicles of T4P-deficient and/or flagellar-deficient strains with wild type strain PAO1. Surprisingly, the Psl-fibre-deficient T4P mutants, such as Δ*pilA* and Δ*pilA*Δ*fliM*, formed pellicles although most of them had less biomass compared with PAO1 (Fig. 5B). The results showed PAO1 formed a flat and dense pellicle with the highest substratum coverage and lowest roughness coefficient (Fig. 5B), an indicator of biofilm heterogeneity (Heydorn *et al.*, 2000). Consistent with the flow cell biofilm data, the pellicle of the Psl-fibre-proficient Δ*fliC* strain had similar biomass as PAO1, but more structure variation indicated by the high roughness (5 times of PAO1) and maximum thickness (3 times of PAO1) (Fig. 5B). The pellicle of the Psl-fibre-deficient Δ*pilA*Δ*fliM* strain had reduced biomass but high roughness, which was similar to the result of flow cell biofilm. In contrast to the flow cell data, the Δ*pilA* strain formed a pellicle that had half of the biomass of PAO1 level while the pellicle of the Δ*pilT* strain was thicker and had slightly more biomass than PAO1. This was consistent with previous suggestion about structural support of T4P in biofilms (Chiang and Burrows, 2003; Barken *et al.*, 2008). Despite this, the pellicles of these two mutants were unstable during the pellicle staining process compared to the wild type pellicle, suggesting loosely bacterial connections within the pellicles of mutants. In addition, the structural support of T4P is not sufficient to promote a stable biofilm in a flow cell as mentioned above (Fig. 5A).

To further investigate the contribution of Psl fibres on maintaining of the pellicle biomass, we performed mannosidase treatment on the PAO1 pellicles as Psl is a mannose-rich polysaccharide (Ma *et al.*, 2007; Byrd *et al.*, 2009). Mannosidase eliminated the most Psl-fibre structure in pellicle and reduce the biomass to 40% of non-treatment control (Fig. 6). This result indicated that the Psl fibre structure was also important for maintaining of pellicle biomass.

In summary, our data indicated that the Psl-fibre matrix played a significant role in efficient biofilm formation, especially at the high shear flow conditions. We conclude that the Psl-fibres may help a biofilm by the following: (i) surrounding multiple-cell aggregates and connecting microcolonies to maintain bacterial association (Figs 1–5 and S1); (ii) acting as web-like backbones that strengthen a biofilm; (iii) recruiting bacteria to join a biofilm by functioning as a structure/surface for T4P to adhere and promote a Psl-derived bacterial community (Figs 1 and 5); and (iv) rapidly covering a surface and efficiently gain biofilm biomass (Figs 2 and 3).

Psl-fibres appear to be formed by Psl released from bacterial surface during T4P-mediated migration

To gain insights into how Psl-fibre strands may form, we stained Psl of bacteria immediately following their attachment to a glass coverslip (green, Fig. 7 upper panels). Psl tracks were observed following bacteria and the length of tracks ranged from 10 to 30 μm (upper panels of Fig. 7, indicated by the white arrow), which is longer than the T4P structure itself (usually ~ 5 μm) (Skerker and Berg, 2001). This suggested that Psl released from bacteria during

migration might form the Psl-fibre strands. We also stained the bacteria with pro-pidium iodide (PI), a red fluorescent dye that stains extracellular DNA (eDNA) or DNA in dying/dead bacteria. The result showed that significant cell death and/or eDNA production occurred in multiple-bacteria aggregates. Moreover, few dead bacteria and visible eDNA were overlapping/associated with Psl tracks suggesting that Psl tracks were derived primarily from living bacteria (Fig. 7, upper merged image).

Psl tracks following bacteria were also observed in Δ*fliC* Psl-overproducing bacteria (Fig. 7, lower panels). Here, Psl-fibre strands appeared to connect two microcolonies and there were a few bacteria joining to the Psl strand (red arrow in Fig. 7 lower panel). A similar phenomenon was also observed in the biofilm of WFPA801 and PAO1 (Figs 1A and S1). Taken together, the above data suggested that Psl released from bacteria during T4P-mediated migration was responsible for forming the Psl-fibre strands.

Starvation triggers Psl release from the bacterial surface and enhances T4P-mediated twitching motility

The radial Psl-fibre matrix was present in the middle of biofilms (Fig. 2E), an area with limited nutrients (Stewart and Franklin, 2008). Thus, we hypothesized that nutrient limitation/starvation may trigger Psl release. To test this, we resuspended bacteria from the mid-log phase culture in either PBS buffer or Jensen's media, and then monitored Psl release during a 5 h period. Our results showed that Psl release from the wild type bacterial surface occurred within 3 h post incubation in PBS (Fig. 8A). In contrast, Psl release was not detected in the samples incubated with Jensen's media although cell-associated Psl was increased during the incubation (Fig. 8A). Psl release in PBS was not a result of bacterial cell death since the bacteria post 5 h of incubation had the same number of live bacteria as the samples at 0 h of incubation (data not shown). Similar Psl release pattern were observed in Psl-overproducing strain WFPA801 (Fig. 8A), indicating the production of Psl did not affect Psl release. These data showed that starvation triggered the Psl release.

To test whether starvation can also induce the T4P-mediated twitching motility, we compared the bacterial twitching ability in Jensen's media agar plate and PBS agar plate. Since bacteria cannot grow in PBS agar, to be able to see the twitching zone, we added 15 ml of middle-log phase culture into a hole with 7 mm diameter and examined the twitching zone surrounding the hole. The twitching zone of PAO1 in PBS plate was double than Jensen's media plate (Figs 8B and S7). This indicated that starvation did enhance T4P-driven twitching motility. We also tested the twitching zone of PAO1 in M9 media and M9 media without carbon source. The results showed that the twitching zones of PAO1 in M9 media were smaller than that of PBS, but larger than that of Jensen's media (Fig. 8B). Depletion of carbon source in M9 media did not show significant impact on the twitching motility. Since the nutrient in M9 media was less rich than Jensen's media, this result indicated poor nutrient can also enhance twitching motility of *P. aeruginosa*. Taken together, our data indicated that starvation can trigger Psl release from bacterial surface as well as T4P-driven bacterial migration. Coupling of these two events may result in the formation of Psl fibres on a surface and in a biofilm.

Discussion

The spider web strategy

One of the most important features of a biofilm is the extracellular polymeric substance that functions as a matrix, holding bacterial cells together. Understanding how a matrix forms may provide therapeutic targets/ strategies to solve biofilm-related problems, such as persistent infections. Up to date, little is known about how a biofilm matrix forms. Psl is a key scaffolding matrix component for *P. aeruginosa* to initiate and maintain biofilms (Matsukawa and Greenberg, 2004; Ma *et al.*, 2006; 2009; 2012; Whitchurch, 2006; Yang *et al.*, 2012). This exopoly-saccharide can form fibre-like strands in biofilm. In this study, we have showed that the Psl fibres connecting to each other results in a spider web-shape matrix. The formation of the fibre-like Psl matrix relies on T4P-driven bacterial migration. Bacterial migration within a biofilm is particularly important as nutrients can quickly become limited within the interiors of the dense cell aggregates in biofilms. Bacteria may benefit by being relocated themselves in the biofilm community in response to changing nutritional gradients. Strikingly, Psl-fibres appear to be formed by Psl released from bacterial surface during T4P-driven bacterial crawling. While T4P drives bacteria forward, Psl tracks appear following bacteria, a strategy similar to the formation of spider web lines. Mutants lacking T4P-mediated twitching motility cannot form the Psl-fibre matrix even if retained T4P on bacterial surface and had a regular Psl release pattern (Figs 4 and S5). This suggests that bacterial migration coupled with Psl polysaccharide release is the key to form a Psl fibre. We have also revealed that starvation can trigger both the T4P-driven bacterial migration and Psl release from bacterial surface, which may couple these two evens. Moreover, we have observed a radial web-like Psl-fibre matrix was present in the middle of both flat flow-cell biofilms and pellicles (Figs 2 and 4), which implies that there is directional bacterial migration occurring in the middle of a biofilm. Importantly, this region of the biofilm is nutrient-deprived (Stewart and Franklin, 2008). In addition, the centre of the radial Psl-fibre matrix is also the centre of a microcolony/dense cell aggregate that have concentrated EPS material including Psl polysaccharide and eDNA/ dead bacteria, suggesting starvation occurred in the centre (Fig. S6). Consistent with this, we observed bacteria moving away from a multiple-cell aggregates that had bacterial cell death occurring (upper panels in Fig. 7, red stain indicates the dead bacteria). These provide a plausible model for how the spider web-like Psl fibres matrix may form. In this model, starvation signals in the centre of bacterial cell aggregates may trigger directional bacterial migration across a substratum/biofilm along with Psl release from bacterial surface, leading to the formation of Psl-fibre strands and the radial pattern Psl-fibre matrix (Fig. 9). The radial Psl-fibre matrix was located in the middle of a flow cell biofilm as well as an air-liquid interface biofilm (pellicle) (Figs 2E and 4; Video S1), suggesting T4P may use matrix material as a surface to mediate bacterial migration within biofilm, which may lead to the connection between Psl fibres and microcolonies (Fig. 9). Since the way that the T4P constructs Psl fibres is similar to form a spider web line and the Psl fibres matrix has spider web look, we therefore named this T4P-dependent Psl fibres matrix formation strategy as spider web strategy.

Pseudomonas aeruginosa depends on two types of appendages (T4P and flagella) for bacterial migration in biofilm, yet they drive bacteria to opposite directions. This may be one of reasons why a *fliC* mutant has more typical radial pattern Psl-fibre matrix in biofilm. Because this mutant totally depends on T4P for bacterial migration, the key player for the Psl-fibre matrix formation as proposed above. As a matter of fact, the wild type strain PAO1 does have a more complex Psl matrix pattern than that of the *fliC* mutant (Fig. 2), which implies that other type of bacterial motility in biofilm may also have some contribution on the formation of Psl matrix.

Rapidly colonizing a surface and biofilm formation is central to bacterial survival among competitors in environmental and clinical settings (Costerton *et al.*, 1995). T4P can function as adhesions for bacteria to rapidly colonize a surface. It can also help bacteria to escape from surfaces when necessary, which is also important for bacterial survival. Psl also promotes surface adherence (Ma *et al.*, 2006), thus Psl release may allow bacteria to rapidly move to a new niches and meanwhile form Psl fibres that help bacterial communities efficiently cover a surface and gain biofilm biomass. The formation of Psl-fibres requires neither the flagella nor other *P. aeruginosa* biofilm matrix polysaccharides such as Pel or alginate. Flagella-deficient strains were often isolated from CF patients (Wolfgang *et al.*, 2004; Lee *et al.*, 2005) and *in vitro* biofilms (the oral presentation of Dr Harrison at 6th ASM Conference on Biofilms, September of 2012). This suggests that flagella-deficient bacteria may benefit biofilm formation. As shown in this study that a flagella deficient strain can utilize T4P-dependent bacterial migration strategy to efficiently form a web-like radial pattern Psl-fibre matrix and a flower-shaped multiple-layer biofilm. This might be the reason for how flagella-deficient bacteria may benefit for biofilm formation. Finally, we showed that Psl-fibres were present in the biofilm of RSCVs, which are also often isolated from CF patients and *in vitro* biofilm (Starkey *et al.*, 2009). Therefore, our data suggest that the T4P-mediated biofilm matrix formation strategy may have general significance for bacterial survival in natural and clinical settings.

Signal molecules involved in Psl release and twitching motility

Starvation-induced polysaccharide release has been reported in marine *Pseudomonas* species (Wrangstadh *et al.*, 1986). Thus, the starvation-triggered exopolysac-charide release may be a general phenomenon. In this report, we have showed that starvation triggers Psl release from the bacterial surface of *P. aeruginosa*. A recent report showed that carbon starvation induced biofilm disperse and cAMP was the signal molecule involved (Huynh *et al.*, 2012). Thus, cAMP might be a possible signal that induces Psl release during carbon starvation. However, carbon starvation does not enhance twitching motility. Consistently, the report of Fulcher and colleagues (2010) also suggested that the control of T4P function was in a cAMP-independent manner. The stringent response (SR) is a regulatory system that allows bacteria to sense and adapt to nutrient-poor environments (Cashel *et al.*, 1996). The RelA and SpoT enzymes-synthesized (p)ppGpp is the central mediator of the SR (Battesti and Bouveret, 2009). Vogt and colleagues reported that the *relAspoT* double mutant of *P. aeruginosa* was defective in swarming and twitching, but not in swimming motility (Vogt *et al.*, 2011). This suggested that (p)ppGpp may be one of signals to regulate starvation-triggered twitching motility, yet this alarmone was not likely involved in the starvation-

induced Psl release as the *relAspoT* mutant exhibited a similar Psl release pattern as PAO1 (Fig. S5). Therefore, cAMP and (p)ppGpp are not the signal molecules coupled Psl release and twitching motility. Future works are required to elucidate which specific signal coupled Psl release and twitching motility, and how the signals regulate these two phenomena.

Summary

Pseudomonas aeruginosa appears to utilize several strategies to build a biofilm matrix. We have previously shown that Psl is arranged in a helical pattern on the bacterial surface and that the interaction between Psl helices on bacteria may help to promote cell–cell interactions and the matrix formation (Ma *et al.*, 2009). In this study, we provide another Psl matrix formation strategy, a T4P-dependent bacterial migration strategy to build a fibre-like Psl matrix through a mechanism similar to that observed for spider web formation. Pilin expression is reported to be repressed in mucoid *P. aeruginosa* (Whitchurch *et al.*, 2002b). Thus, alginate-derived bio-films are unlikely to use T4P-mediated migration to form a fibre-like matrix of alginate. A specific staining reagent for Pel has not been developed, so we were unable to determine whether Pel-rich biofilms rely on T4P-mediated bacterial migration.

T4P participate in a number of fundamental bacterial processes, including motility, fruiting body formation, adherence to surfaces/host cells, and biofilm formation (Strom and Lory, 1993). In this report, we gain insight into how T4P participate in the formation of a Psl fibre matrix during biofilm development. In *Myxococcus xanthus*, extracellular polysaccharides mediate pilus retraction and T4P-mediated social-motility promotes fruiting body formation (Mauriello *et al.*, 2010). In *P. aeruginosa*, Psl is not necessary for T4P-mediated twitching motility (Table 1), but T4P-mediated motility can help to build a fibre-like Psl polysaccharide matrix within biofilms. Most strikingly, starvation signals can couple Psl release and T4P-mediated twitching motility, leading to the formation of Psl-fibre matrix. Recently, Nguyen and colleagues reported that starvation responses mediated antibiotic tolerance in biofilms and nutrient-limited bacteria (Nguyen *et al.*, 2011). Thus the starving bacteria appear to outperform in biofilm formation and persistence during infections and survival in the environment.

The T4P are present in several biofilm forming bacteria, such as *Neisseria gonorrhoeae, N. meningitidis, Vibrio cholerae, Legionella pneumophila, Salmonella enterica* and enteropathogenic *E. coli* (Strom and Lory, 1993). Future work may provide evidence that T4P-dependent biofilm matrix formation strategy is a general mechanism conserved in the T4P-producing bacteria.

Experimental procedures

Strains and growth conditions

Pseudomonas aeruginosa strains used in this study and their motility phenotype are listed in Table 1. P_{BAD}-*psl* strains, WFPA802 and IMPA13 were constructed by the exactly same unmarked in-frame deletion strategy used for WFPA801 as described previously (Hoang *et al.*, 1998; Ma *et al.*, 2006). The IMPA34(Δ*fliC*Δ*pilT*), IMPA33(Δ*pilT*) and IMPA31(Δ*pilH*)

were constructed by the unmarked in-frame deletion strategy (Hoang *et al.*, 1998), whereby DNA encoding amino acid 5–486 of FliC and/or 4–342 of PilT, and the entire encoded region of *pilH* were deleted respectively. Unless otherwise indicated, *P. aeruginosa* was grown at 37°C in Luria–Bertani medium lacking sodium chloride (LBNS) or Jensen's, a chemically defined medium (Jensen *et al.*, 1980). Biofilms of *P. aeruginosa* were cultured in Jensen's medium at room temperature (RT) (Ma *et al.*, 2006). To induce the transcription of the *psl* operon, 2% arabinose was added to Jensen's medium.

Immunoblotting of Psl polysaccharide extracts

Bacteria were collected from 450 μl of culture (OD_{600}~0.5). Pellets were resuspended with 450 μl PBS buffer or Jensen's media and incubated at the RT for 1–5 h. At each hour, Psl was extracted from bacteria and culture supernatant. Bacterial surface-associated Psl was extracted as previously described (Byrd *et al.*, 2009). Released Psl in the supernatant was precipitated by 3 volumes of 100% ethanol, resuspended in 50 μl 0.5 M EDTA and treated with proteinase K for 1 h. Psl extracts were detected by immunoblotting with anti-Psl serum as described previously (Byrd *et al.*, 2009).

Biofilm and Psl matrix staining

The air-liquid interface biofilms were grown in glass chambers (Chambered #1.5 German Coverglass System, Nunc) with glass coverslip at the bottom. Mannosidase (Sigma, 10 u per chamber) was added into glass chambers 1 h post inoculation. For CLSM observation, buffers were gently sucked out from glass chambers to allow pellicles to drop down on the coverslips. The flow cell biofilms were grown at RT in three-channel flow cell with individual channel dimensions of 1 × 4 × 40 mm (Stovall Life Science) as previously described (Ma *et al.*, 2006). The mid-log phase culture was used for inoculation. The biofilms were stained by membrane stain FM4-64 (1 μm final concentration, Molecular Probes, Invitrogen) or DNA stain SYTO9 (Molecular Probes, Invitrogen). Psl matrix was stained by fluorescence-labelled lectin HHA at 100 μg ml^{-1} (EY lab) as we described elsewhere (Ma *et al.*, 2009).

Psl and PI staining for surface-attached bacteria

Psl expression of WFPA801 and IMPA13 was induced by addition of 2% arabinose for 3 h at 37°C with shaking, 0.5 ml of these cultures was utilized to inoculate glass chambers respectively (Chambered #1.5 German Coverglass System, Nunc). After 1 h of incubation at RT, the bacteria attached on glass coverslip were stained with lectin HHA-FITC for 2 h at RT and stained by PI (Invitrogen) for 10 min in dark.

Microscopy and image acquisition

All fluorescent images were acquired by a Zeiss 510 CLSM (Carl Zeiss, Jena, Germany). Images were obtained using 63×/1.3 objective. A LSM image browser generated the 3D images and optical Z-sections. CLSM-captured images were subjected to quantitative image analysis using *COMSTAT* software as previously described (Heydorn *et al.*, 2000). The Psl fluorescence intensity of PAO1 and Δ*pilA* strains were analysed by using Interactive 3D Surface Plot plugin of ImageJ software (version 1.43u, NIH).

Motility assay

Twitching motility was assayed by stab inoculating strains through a thin LBNS/Jensens's media agar (1% w/v) plate with 24–48 h of incubation at 30°C under humidified condition. Twitching zones were visualized at the agar plate interface (Whitchurch *et al.*, 2002b). Flagellum-mediated swimming motility was assayed by stab inoculating strains onto LBNS agar plates (0.3% agar). After 24 h of incubation at 37°C, motility was assessed by measuring the diameters of the circular zones that the colonies spread from their points of inoculation (Arora *et al.*, 1998). For starvation-induced twitching assay, a 7 mm-diameter hole was obtained on a 1.0% agar plate in Jensen's media or PBS containing 0.1% tetrazolium red respectively. The 15 ml of mid-log phase culture was inoculated into the holes and the twitch zone was measured after 48 h of incubation at 30°C. In order to assay the influence of carbon source depletion on twitching, M9 media with or without carbon was used under the same condition. All data were obtained from three independent experiments.

Supplementary Material

Refer to Web version on PubMed Central for supplementary material.

Acknowledgements

We thank Dr Tolker-Nielsen at University of Copenhagen for providing the Δ*fliM*Δ*pilA* strain, Dr Engel at University of California for *pilH*, and *pilT* mutant strains, Dr Nguyen at McGrill University for *relAspoT* mutant, and Dr Di Wang, Dr Qing Wei and Dr Palashpriya Das at Institute of Microbiology, Chinese Academy of Sciences for help in English writing. This work was supported by Chinese Academy of Science grant KSCXZ-YW-BR-5 (L.M.), National Natural Science Foundation of China grant 31270177 and 31140041 (L.M.), and Public Health Service grants AI061396 and HL058334 (D.J.W.), USA.

References

Arora SK, Ritchings BW, Almira EC, Lory S, Ramphal R. The *Pseudomonas aeruginosa* flagellar cap protein, FliD, is responsible for mucin adhesion. Infect Immun. 1998; 66:1000–1007. [PubMed: 9488388]

Barken KB, Pamp SJ, Yang L, Gjermansen M, Bertrand JJ, Klausen M, et al. Roles of type IV pili, flagellum-mediated motility and extracellular DNA in the formation of mature multicellular structures in *Pseudomonas aeruginosa* biofilms. Environ Microbiol. 2008; 10:2331–2343. [PubMed: 18485000]

Battesti A, Bouveret E. Bacteria possessing two RelA/SpoT-like proteins have evolved a specific stringent response involving the acyl carrier protein-SpoT interaction. J Bacteriol. 2009; 191:616–624. [PubMed: 18996989]

Bertrand JJ, West JT, Engel JN. Genetic analysis of the regulation of type IV pilus function by the Chp chemosensory system of *Pseudomonas aeruginosa*. J Bacteriol. 2010; 192:994–1000. [PubMed: 20008072]

Byrd MS, Sadovskaya I, Vinogradov E, Lu H, Sprinkle AB, Richardson SH, et al. Genetic and biochemical analyses of the *Pseudomonas aeruginosa* Psl exopoly-saccharide reveal overlapping roles for polysaccharide synthesis enzymes in Psl and LPS production. Mol Microbiol. 2009; 73:622–638. [PubMed: 19659934]

Byrd MS, Pang B, Mishra M, Swords WE, Wozniak DJ. The *Pseudomonas aeruginosa* exopolysaccharide Psl facilitates surface adherence and NF-κB activation in A549 Cells. mBio. 2010; 1:e00140–e00110. [PubMed: 20802825]

Cashel, M.; Gentry, D.; Hernandez, VJ.; Vinella, D. The stringent response. In: Neidhardt, FC.; Curtiss, R., III; Ingraham, JL.; Lin, ECC.; Low, KB.; Magasanik, B., et al., editors. *Escherichia coli*

and *Salmonella typhimurium*: Cellular and Molecular Biology. Washington, DC, USA: ASM Press; 1996. p. 1458-1496.

Chiang P, Burrows LL. Biofilm formation by hyperpiliated mutants of *Pseudomonas aeruginosa*. J Bacteriol. 2003; 185:2374–2378. [PubMed: 12644510]

Colvin KM, Gordon VD, Murakami K, Borlee BR, Wozniak DJ, Wong GCL, et al. The Pel polysaccharide can serve a structural and protective role in the biofilm matrix of *Pseudomonas aeruginosa*. PLoS Pathog. 2011; 7:e1001264. [PubMed: 21298031]

Conrad JC, Gibiansky ML, Jin F, Gordon VD, Motto DA, Mathewson MA, et al. Flagella and pili-mediated near-surface single-cell motility mechanisms in *P. aeruginosa*. Biophys J. 2011; 100:1608–1616. [PubMed: 21463573]

Costerton JW, Lewandowski Z, Caldwell DE, Korber DR, Lappin-Scott HM. Microbial Biofilms. Annu Rev Microbiol. 1995; 49:711–745. [PubMed: 8561477]

Costerton JW, Stewart PS, Greenberg EP. Bacterial biofilms: a common cause of persistent infections. Science. 1999; 284:1318–1322. [PubMed: 10334980]

Davies DG, Parsek MR, Pearson JP, Iglewski BH, Costerton JW, Greenberg EP. The involvement of cell-to-cell signals in the development of a bacterial biofilm. Science. 1998; 280:295–298. [PubMed: 9535661]

Flemming HC, Wingender J. The biofilm matrix. Nat Rev Microbiol. 2010; 8:623–633. [PubMed: 20676145]

Friedman L, Kolter R. Genes involved in matrix formation in *Pseudomonas aeruginosa* PA14 biofilms. Mol Microbiol. 2004a; 51:675–690. [PubMed: 14731271]

Friedman L, Kolter R. Two genetic loci produce distinct carbohydrate-rich structural components of the *Pseudomonas aeruginosa* biofilm matrix. J Bacteriol. 2004b; 186:4457–4465. [PubMed: 15231777]

Fulcher NB, Holliday PM, Klem E, Cann MJ, Wolfgang MC. The *Pseudomonas aeruginosa* Chp chemosensory system regulates intracellular cAMP levels by modulating adenylate cyclase activity. Mol Microbiol. 2010; 76:889–904. [PubMed: 20345659]

Govan JRW, Deretic V. Microbial pathogenesis in cystic fibrosis: mucoid *Pseudomonas aeruginosa* and *Burkholderia cepacia*. Microbiol Rev. 1996; 60:539–574. [PubMed: 8840786]

Hentzer M, Teitzel GM, Balzer GJ, Heydorn A, Molin S, Givskov M, et al. Alginate overproduction affects *Pseudomonas aeruginosa* biofilm structure and function. J Bacteriol. 2001; 183:5395–5401. [PubMed: 11514525]

Heydorn A, Nielsen AT, Hentzer M, Sternberg C, Givskov M, Ersboll BK, et al. Quantification of biofilm structures by the novel computer program *COMSTAT*. Microbiology. 2000; 146:2395–2407. [PubMed: 11021916]

Hoang TT, Karkhoff-Schweizer RR, Kutchma AJ, Schweizer HP. A broad-host-range Flp-*FRT* recombination system for site-specific excision of chromosomally-located DNA sequences: applications for isolation of unmarked *Pseudomonas aeruginosa* mutants. Gene. 1998; 212:77–86. [PubMed: 9661666]

Huynh TT, McDougald D, Klebensberger J, Al Qarni B, Barraud N, Rice SA, et al. Glucose starvation-induced dispersal of *Pseudomonas aeruginosa* biofilms is cAMP and energy dependent. PLoS ONE. 2012; 7:e42874. [PubMed: 22905180]

Jensen SE, Fecycz IT, Campbell JN. Nutritional factors controlling exocellular protease production by *Pseudomonas aeruginosa*. J Bacteriol. 1980; 144:844–847. [PubMed: 6776099]

Kirisits MJ, Prost L, Starkey M, Parsek MR. Characterization of colony morphology variants isolated from *Pseudomonas aeruginosa* biofilms. Appl Environ Microbiol. 2005; 71:4809–4821. [PubMed: 16085879]

Klausen M, Aaes-Jorgensen A, Molin S, Tolker-Nielsen T. Involvement of bacterial migration in the development of complex multicellular structures in *Pseudomonas aeruginos*a biofilms. Mol Microbiol. 2003a; 50:61–68. [PubMed: 14507363]

Klausen M, Heydorn A, Ragas P, Lambertsen L, Aaes-Jorgensen A, Molin S, et al. Biofilm formation by *Pseudomonas aeruginosa* wild type, flagella and type IV pili mutants. Mol Microbiol. 2003b; 48:1511–1524. [PubMed: 12791135]

Kohler T, Curty LK, Barja F, van Delden C, Pechere JC. Swarming of *Pseudomonas aeruginosa* is dependent on cell-to-cell signaling and requires flagella and pili. J Bacteriol. 2000; 182:5990–5996. [PubMed: 11029417]

Kolodkin-Gal I, Romero D, Cao S, Clardy J, Kolter R, Losick R. D-amino acids trigger biofilm disassembly. Science. 2010; 328:627–629. [PubMed: 20431016]

Kolodkin-Gal I, Cao S, Chai L, Böttcher T, Kolter R, Clardy J, et al. A self-produced trigger for biofilm disassembly that targets exopolysaccharide. Cell. 2012; 149:684–692. [PubMed: 22541437]

Lee B, Haagensen JAJ, Ciofu O, Andersen JB, Hoiby N, Molin S. Heterogeneity of biofilms formed by nonmucoid *Pseudomonas aeruginosa* isolates from patients with cystic fibrosis. J Clin Microbiol. 2005; 43:5247–5255. [PubMed: 16207991]

Lewis K. Persister cells, dormancy and infectious disease. Nat Rev Microbiol. 2007; 5:48–56. [PubMed: 17143318]

Ma L, Jackson K, Landry RM, Parsek MR, Wozniak DJ. Analysis of *Pseudomonas aeruginosa* conditional Psl variants reveals roles for the Psl polysaccharide in adhesion and maintaining biofilm structure postattachment. J Bacteriol. 2006; 188:8213–8221. [PubMed: 16980452]

Ma L, Lu H, Sprinkle A, Parsek MR, Wozniak DJ. *Pseudomonas aeruginosa* Psl is a galactose- and mannose-rich exopolysaccharide. J Bacteriol. 2007; 189:8353–8356. [PubMed: 17631634]

Ma L, Conover M, Lu H, Parsek MR, Bayles K, Wozniak DJ. Assembly and development of the *Pseudomonas aeruginosa* biofilm matrix. PLoS Pathog. 2009; 5:e1000354. [PubMed: 19325879]

Ma L, Wang S, Wang D, Parsek MR, Wozniak DJ. The roles of biofilm matrix polysaccharide Psl in mucoid *Pseudomonas aeruginosa* biofilms. FEMS Immunol Med Microbiol. 2012; 65:377–380. [PubMed: 22309106]

Mah TF, Pitts B, Pellock B, Walker GC, Stewart PS, O'Toole GA. A genetic basis for *Pseudomonas aeruginosa* biofilm antibiotic resistance. Nature. 2003; 426:306–310. [PubMed: 14628055]

Matsukawa M, Greenberg EP. Putative exopolysaccharide synthesis genes influence *Pseudomonas aeruginosa* biofilm development. J Bacteriol. 2004; 186:4449–4456. [PubMed: 15231776]

Mauriello EMF, Mignot T, Yang Z, Zusman DR. Gliding motility revisited: how do the *Myxobacteria* move without flagella? Microbiol Mol Biol Rev. 2010; 74:229–249. [PubMed: 20508248]

Nguyen D, Joshi-Datar A, Lepine F, Bauerle E, Olakanmi O, Beer K, et al. Active starvation responses mediate antibiotic tolerance in biofilms and nutrient-limited bacteria. Science. 2011; 334:982–987. [PubMed: 22096200]

O'Toole GA, Kolter R. Flagellar and twitching motility are necessary for *Pseudomonas aeruginosa* biofilm development. Mol Microbiol. 1998; 30:295–304. [PubMed: 9791175]

Shrout JD, Chopp DL, Just CL, Hentzer M, Givskov M, Parsek MR. The impact of quorum sensing and swarming motility on *Pseudomonas aeruginosa* biofilm formation is nutritionally conditional. Mol Microbiol. 2006; 62:1264–1277. [PubMed: 17059568]

Shrout JD, Tolker-Nielsen T, Givskov M, Parsek MR. The contribution of cell-cell signalling and motility to bacterial biofilm formation. MRS Bull. 2011; 36:367–373. [PubMed: 22053126]

Singh PK, Schaefer AL, Parsek MR, Moninger TO, Welsh MJ, Greenberg EP. Quorum-sensing signals indicate that cystic fibrosis lungs are infected with bacterial biofilms. Nature. 2000; 407:762–764. [PubMed: 11048725]

Skerker JM, Berg HC. Direct observation of extension and retraction of type IV pili. Proc Natl Acad Sci USA. 2001; 98:6901–6904. [PubMed: 11381130]

Starkey M, Hickman JH, Ma L, Zhang N, De Long S, Hinz A, et al. *Pseudomonas aeruginosa* rugose small-colony variants have adaptations that likely promote persistence in the cystic fibrosis lung. J Bacteriol. 2009; 191:3492–3503. [PubMed: 19329647]

Stewart PS, Franklin MJ. Physiological heterogeneity in biofilms. Nat Rev Microbiol. 2008; 6:199–210. [PubMed: 18264116]

Strom MS, Lory S. Structure-function and biogenesis of the type IV pili. Annu Rev Microbiol. 1993; 47:565–596. [PubMed: 7903032]

Sutherland IW. The biofilm matrix - an immobilized but dynamic microbial environment. Trends Microbiol. 2001; 9:222–227. [PubMed: 11336839]

Vogt SL, Green C, Stevens KM, Day B, Erickson DL, Woods DE, et al. The stringent response is essential for *Pseudomonas aeruginosa* virulence in the rat lung agar bead and *Drosophila melanogaster* feeding models of infection. Infect Immun. 2011; 79:4094–4104. [PubMed: 21788391]

Watson AA, Mattick JS, Alm RA. Functional expression of heterologous type 4 fimbriae in *Pseudomonas aeruginosa*. Gene. 1996; 175:143–150. [PubMed: 8917091]

Whitchurch, CB. Biogenesis and function of type IV pillin in *Pseudomonas* species. In: Ramos, JL.; Levesque, RC., editors. Pseudomonas. Vol. 4. USA: Springer US; 2006. p. 139-188.

Whitchurch CB, Tolker-Nielsen T, Ragas PC, Mattick JS. Extracellular DNA required for bacterial biofilm formation. Science. 2002a; 295:1487. [PubMed: 11859186]

Whitchurch CB, Erova TE, Emery JA, Sargent JL, Harris JM, Semmler ABT, et al. Phosphorylation of the *Pseudomonas aeruginosa* response regulator AlgR is essential for type IV fimbria-mediated twitching motility. J Bacteriol. 2002b; 184:4544–4554. [PubMed: 12142425]

Willcox MD. *Pseudomonas aeruginosa* infection and inflammation during contact lens wear: a review. Optom Vis Sci. 2007; 84:273–278. [PubMed: 17435510]

Wolfgang MC, Jyot J, Goodman AL, Ramphal R, Lory S. *Pseudomonas aeruginosa* regulates flagellin expression as part of a global response to airway fluid from cystic fibrosis patients. Proc Natl Acad Sci USA. 2004; 101:6664–6668. [PubMed: 15084751]

Wozniak DJ, Sprinkle AB, Baynham PJ. Control of *Pseudomonas aeruginosa algZ* expression by the alternative sigma factor AlgT. J Bacteriol. 2003; 185:7297–7300. [PubMed: 14645293]

Wrangstadh M, Conway PL, Kjelleberg S. The production and release of an extracellular polysaccharide during starvation of a marine *Pseudomonas sp*. and the effect thereof on adhesion. Arch Microbiol. 1986; 145:220–227. [PubMed: 3767571]

Yang L, Hu Y, Liu Y, Zhang J, Ulstrup J, Molin S. Distinct roles of extracellular polymeric substances in *Pseudomonas aeruginosa* biofilm development. Environ Microbiol. 2011; 3:1705–1717. [PubMed: 21605307]

Yang L, Wang H, Wu H, Damkiær S, Jochumsen N, Song Z, et al. Polysaccharides serve as scaffold of biofilms formed by mucoid *Pseudomonas aeruginosa*. FEMS Immunol Med Microbiol. 2012; 65:366–376. [PubMed: 22309122]

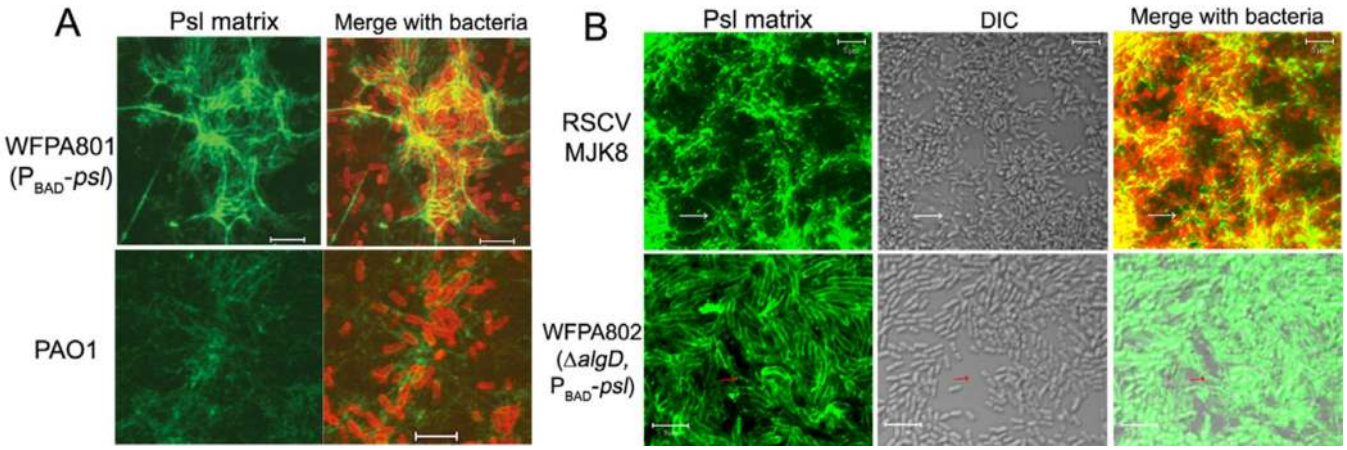

Fig. 1.

Spider-web-like Psl-fibre matrixes in the biofilms of a variety of *P. aeruginosa* PAO1-derived strains. Shown are biofilms of PAO1 (A), Psl-inducible strain WFPA801 (A), RSCV MJK8 (B) and Δ*algD* Psl-inducible strain WFPA802 (B) after 22 h of growth under flow condition and stained with HHA-FITC (green, Psl matrix) and FM4-64 (red, bacteria membrane stain). Grey images are corresponding differential interference contrast (DIC) image of biofilms. Merged images were either merge of Psl matrix (green) with FM4-64 labelled biofilm (red) or with DIC image (lower right image in B). Arrows indicate the Psl-fibres located on the area with few bacteria. Scale bar: 2 μm for biofilm images of PAO1 and WFPA801, 5 μm for MJK8 and WFPA802.

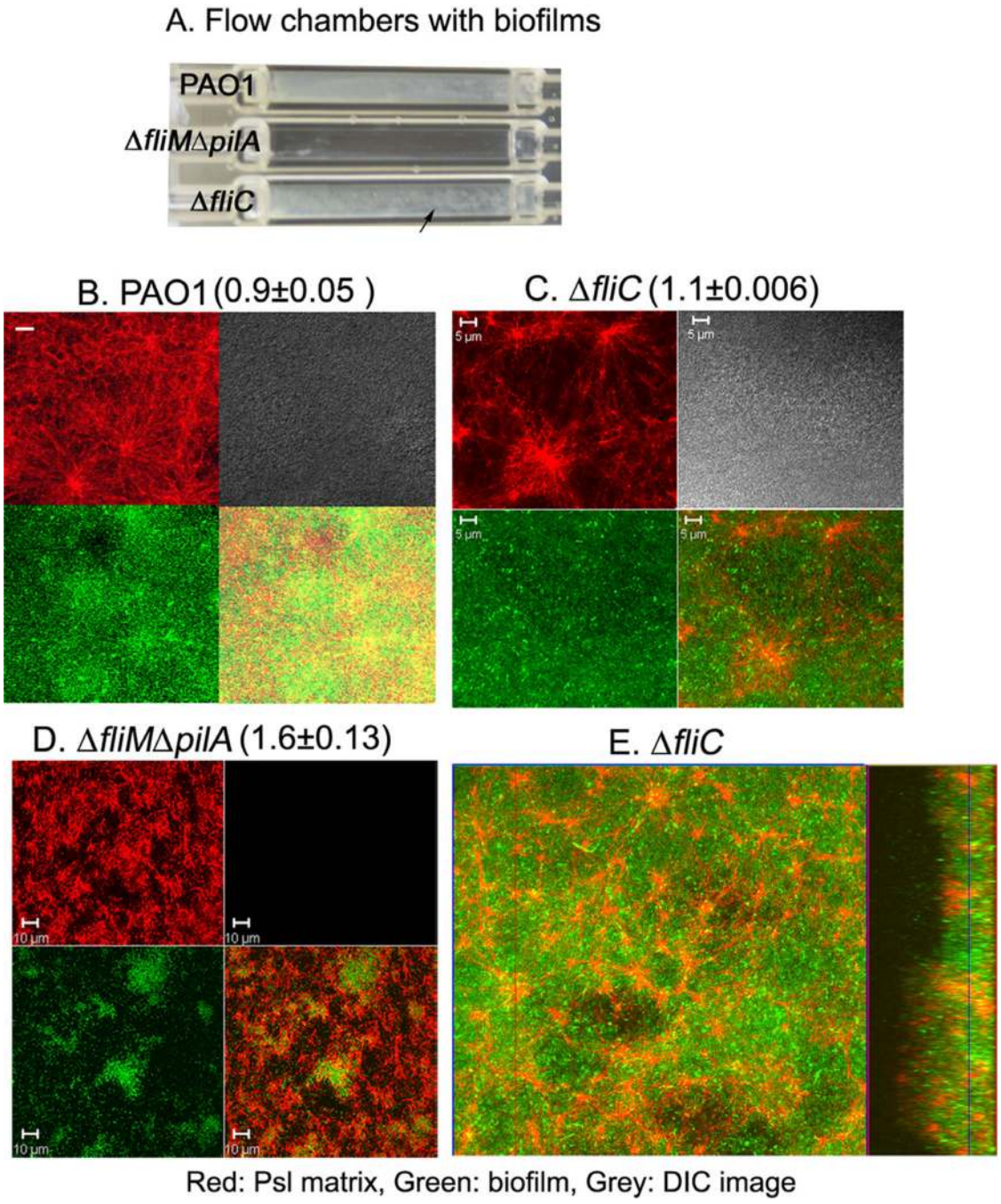

Fig. 2.

Type IV pili are necessary for the formation of the Psl-fibre matrix.

A. Photograph of a flow cell with the 4-day-old biofilms of strain PAO1, Δ*fliM*Δ*pilA* and Δ*fliC*. The black arrow indicates the irregular-shaped large macrocolonies.

B–D. Shown are selected CLSM images of the flow cell biofilms (green) and the corresponding Psl matrix (red). Psl matrix was stained by HHA-TRITC (red). The bacteria in the Δ*fliC* biofilms were stained by SYTO9 (green) and the Δ*fliM*Δ*pilA* mutant was

labelled by GFP. The lower right images of each panel were merged image of green (bacteria in biofilms) and red (matrix).

E. A selected optical section image (large square) showed how the web-like radial pattern Psl-fibre matrix (red) enmeshed bacteria in the biofilm (green) of a Δ*fliC* strain. The blue line on the rectangle image shows the section located in the middle of biofilm, which is depicted in the large square. Scale bar: 5 μm for PAO1 and Δ*fliC*, 10 μm for Δ*fliM*Δ*pilA*. The numbers with deviation above the images B–D indicated the Psl relative to biofilm biomass.

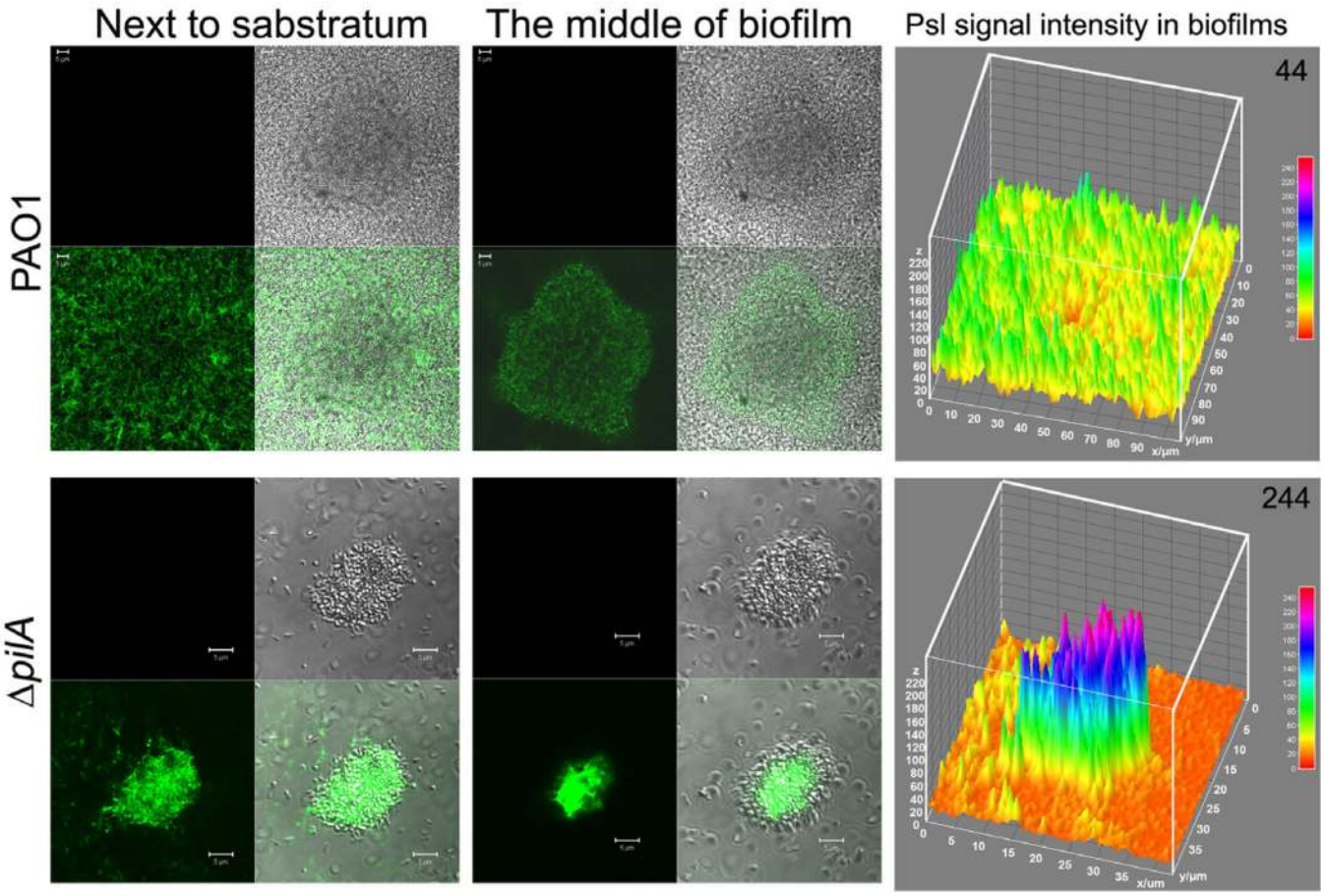

Fig. 3.

The biofilm microcolonies and Psl matrix of *P. aeruginosa* PAO1 and its isogenic Δ*pilA* mutant. Shown are selected optical sectioned images of PAO1 and Δ*pilA* biofilms stained by HHA-FITC after 3 days of growth in a flow cell. The lower right small square images at the left and middle panels are merged images of corresponding green (Psl) and DIC (biofilm) image. Scale bar, 5 μm. The right panel images depict the Psl fluorescence intensity in the corresponding biofilm. The average Psl signal intensity in per μm^3 biofilm is shown at the upper right corner of the corresponding image.

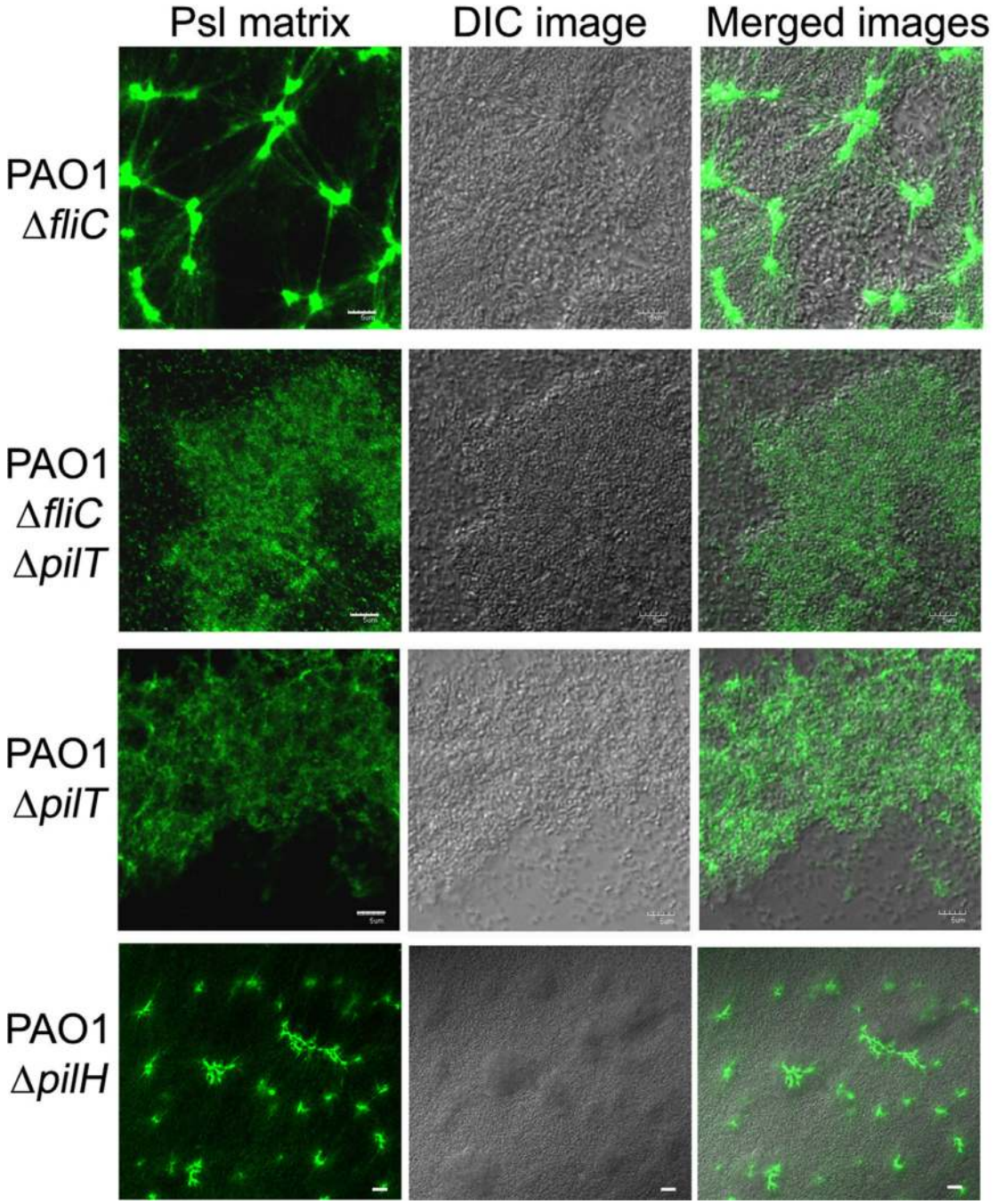

Fig. 4.

The Psl matrix in the pellicles of Δ*fliC*, Δ*fliC*Δ*pilT*, Δ*pilT* and Δ*pilH* strain. Shown are selected CLSM images located in the middle of pellicles. The pellicles were stained by FITC-HHA for Psl matrix (green) after 44 h of growth under a static growth condition. Grey image was the corresponding DIC image of biofilm. Scale bar, 5 μm for all images.

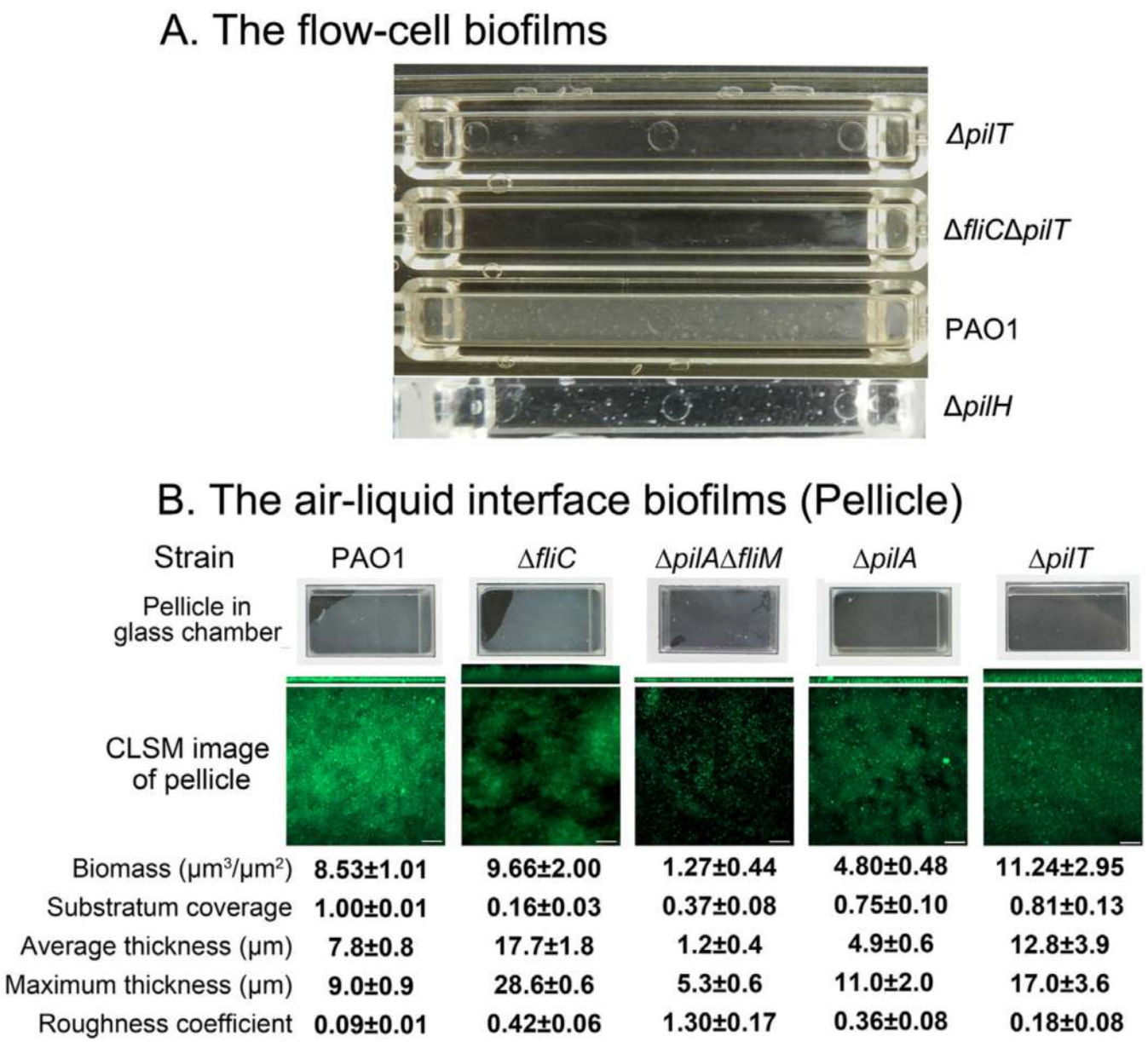

Fig. 5.

The contribution of Psl fibres in the biofilm formation.

A. A photograph of flow cells with the 2-day-old biofilms of strain PAO1 and T4P mutants. The white cloud and spot in the lower two chambers indicate biofilms and microcolonies.

B. The pellicles of PAO1 and PAO1-derived T4P mutants. The pellicles are stained by SYTO9 (green). The upper panel shows the photos of glass chamber with pellicles. The lower panel show representative 3-dimesion-reconstructed CLSM image of each pellicle. Squares are top-down view and rectangles are side view. A *COMSTAT* analysis of the data from each pellicle is indicated below.

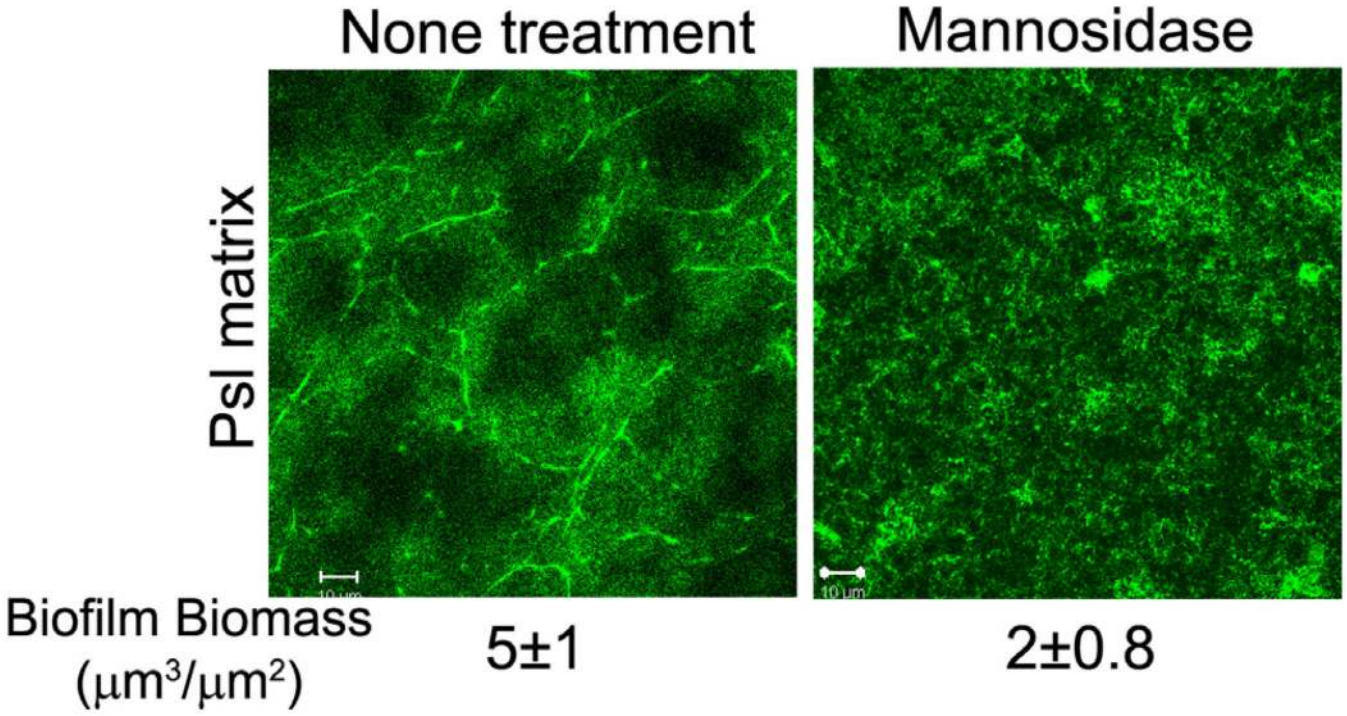

Fig. 6.

Mannosidase treatment eliminates the Psl fibres and reduces biofilm biomass. Shown are the HHA-FITC stained Psl matrix of PAO1 pellicles with/without mannosidase treatment. Corresponding biomass are shown under the images. Scale bar, 10 μm.

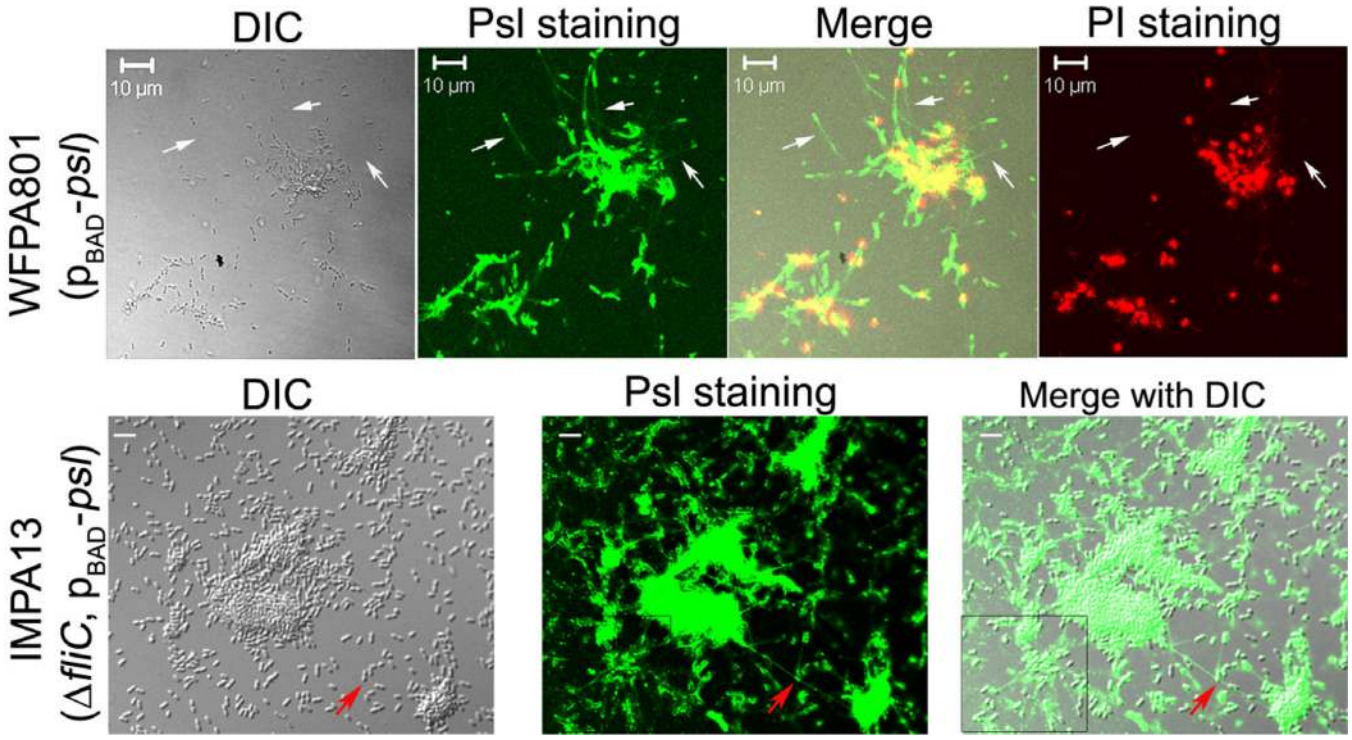

Fig. 7.

Psl tracks were detected after bacterial cells attached on a glass slip. Shown are surface-attached bacterial cells of WFPA801 and IMPA13 stained by HHA-FITC and/or propidium iodide (PI). White arrows pointed out the HHA-FITC stained Psl tracks (green) following bacterial cells. Red fluorescent signals were PI stained DNA of dead/dying bacteria. The red arrow indicates a Psl-fibre strand connecting two microcolonies. The boxed area showed the web-like radial pattern Psl tracks. Grey panel was the corresponding DIC image. Scale bar: 10 mm for WFPA801, 5 μm for IMPA13.

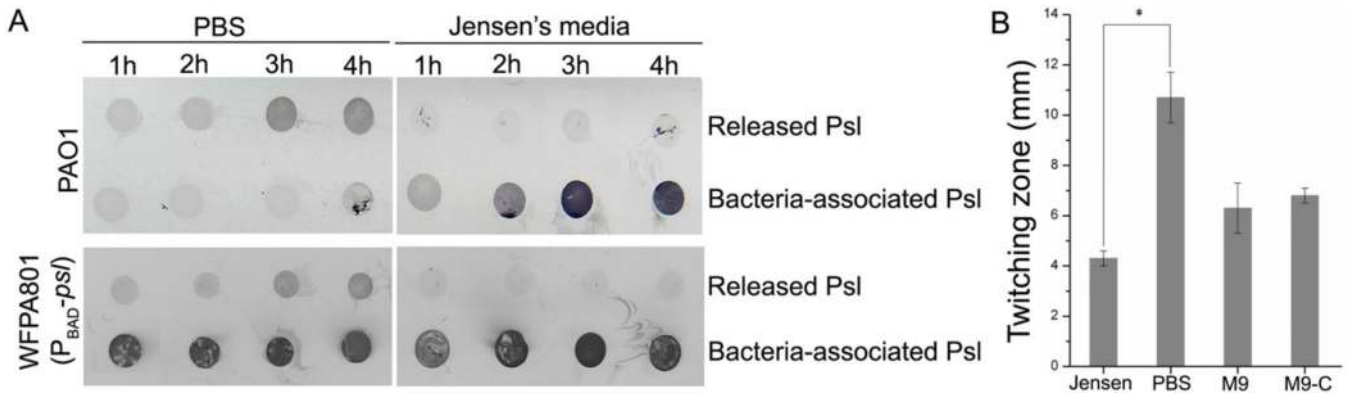

Fig. 8.

Psl release and twitching motility of *P. aeruginosa* strains under different nutrient conditions.

A. Psl released into PBS buffer and Jensen's media from mid-log phase bacteria of PAO1 and the Psl-overproducing strain WFPA801 during 4 h of incubation at RT. Released Psl and bacterial surface-associated Psl were detected by immunoblotting with anti-Psl serum.

B. The twitching zone of PAO1 on the Jensen's media agar plate, PBS agar plate, M9 media plates and M9 media without carbon source (M9-C). **P* < 0.001 (one-way ANOVA).

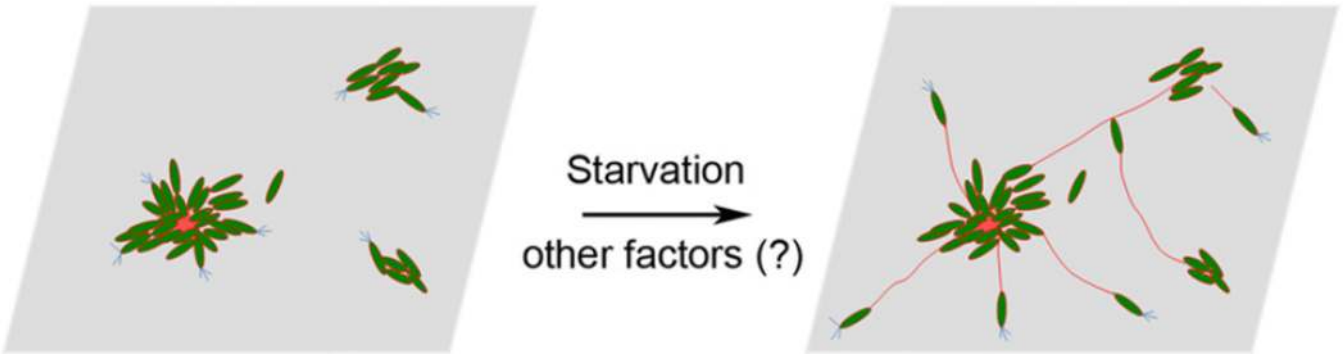

Fig. 9.

A model for how a radial pattern Psl-fibre matrix may form. Starvation within a multiple-cell aggregate triggers Psl polysaccharide release from the bacteria surface and T4P-mediated bacterial migration, resulting in a radial web-like Psl-fibre matrix. Psl and Psl-fibres may function as a structure/surface for T4P to recruit bacteria to join a matrix or biofilm. Green, bacteria; red, Psl; blue, T4P.

Table 1

The strains used in this study and their motility phenotype.

***P. aeruginosa* PAO1-derived strains**	**Relevant characteristics**	**Swimming[a]**	**Twitching[b]**	**Source/reference**
PAO1	Non-mucoid, wild type strain,	++	++	
MJK8	Rugose small-colony variant, isolated from aged biofilm of PAO1.	–	–	Kirisits *et al.* (2005)
MJK8-D*pel*	MJK8 Δ*pel*	–	–	Kirisits *et al.* (2005)
MJK8-D*psl*	MJK8 Δ*psl*	+	±	Kirisits *et al.* (2005)
WFPA801	*psl*-inducible strain, P_{BAD}-*psl*	++	++	Ma *et al.* (2006)
WFPA1	Δ*algD*, Tc^r	++	++	Wozniak *et al.* (2003)
WFPA802	Δ*algD*, P_{BAD}-*psl*, Tc^r	++	++	This study
WFPA850	Δ*fliC*, in frame no mark deletion strain	–	++	Byrd *et al.* (2010)
Δ*fliM*Δ*pilA*	Gfp-tagged PAO1, Δ*fliM*Δ*pilA*,	–	–	Klausen *et al.* (2003b)
Δ*relA*Δ*spoT*	*relA* and *spoT* double deletion mutant	ND	ND	Nguyen *et al.* (2011)
AWO	Δ*pilA*	++	–	Watson *et al.* (1996)
IMPA31	In-frame deletion of *pilH*	++	+	This study
IMPA33	In-frame deletion of *pilT*	+	–	This study
IMPA13	Δ*fliC*, P_{BAD}-*psl*	–	++	This study
IMPA34	In-frame deletion of *fliC* and *pilT*	–	–	This study

a. ++, motility zone ≥20 mm; +, motility zone ≥10 mm; –, no motility zone/the zone similar to negative control.

b. ++, motility zone ≥15 mm; +, 40–60% of wt motility zone; ±, < 40% of wt motility zone; –, no motility zone/the zone similar to negative control.

ND, not done.